Optical Materials 47 (2015) 211–218

Contents lists available at ScienceDirect

Optical Materials

journal homepage: www.elsevier.com/locate/optmat

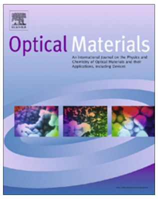

The nonlinear absorption in new lanthanide double decker pyridine-based phthalocyanines in solution and thin films

Kutloano Edward Sekhosana, Tebello Nyokong *

Department of Chemistry, Rhodes University, PO Box 94, Grahamstown 6140, South Africa

ARTICLE INFO

Article history:
Received 5 March 2015
Received in revised form 18 April 2015
Accepted 5 May 2015
Available online 3 June 2015

Keywords:
Optical behavior
Susceptibility
Hyperpolarization
Threshold
Nonlinear
Transmission

ABSTRACT

The optical behavior of bis-{2(3), 9(10), 16(17), 23(24)-(tetrapyridin-4-yloxy phthalocyaninato)} lanthanum (III) (**2**) and its ytterbium (**3**) counterpart in dimethyl sulfoxide are presented and compared to bis-{1(4), 8(11), 15(18), 22(25)-(tetrapyridin-4-yloxy phthalocyaninato)} ytterbium (III) (**4**). We report on the third-order susceptibility, second-order hyperpolarizability and the limiting threshold values. The nonlinear optical limiting threshold values of complexes **2**, **3** and **4** showed improvement in the solid state (thin films), with complex **4** giving the best value at 0.033 J cm^{-2}.

1. Introduction

Bis(phthalocyaninato) lanthanide (LnPc$_2$) complexes are interesting due to their unique physical, spectroscopic and electrochemical properties [1]. LnPc$_2$ complexes have applications in many areas such as in nonlinear optics (NLO) [2–4], effect transistors, molecular magnets, molecular-based multibit information storage materials, receptors for metal ions and saccharides, and molecular solar cells [5–11]. LnPc$_2$ complexes exhibit high reverse saturable absorption (RSA) [12,13] due to extensive π-electron system caused by π–π interaction of two Pc macrocyclic rings coordinated to a lanthanide ion. However, the NLO studies of LnPc$_2$ complexes are still limited [2–4,14,15]. We have recently reported on the NLO behavior of bis-{1(4), 8(11), 15(18), 22(25)-(tetrapyridin-4-yloxy phthalocyaninato)} ytterbium (III) (complex **4** in Scheme 1) which is substituted with pyridin-4-yloxy groups at the non-peripheral positions [16]. Substitution at non-peripheral positions is expected to reduce aggregation and improve photophysical parameters. Liu et al. [17] examined indium phthalocyanine, both in solution and in a polymer film, and observed a significant increase in optical limiting ability along with observations of phthalocyanine aggregation in the polymer film. In this work we compare the NLO behavior of non-peripherally substituted complex **4**, with that of the peripherally substituted bis-{2(3), 9(10), 16(17), 23(24)-(tetrapyridin-4-yloxy phthalocyaninato)} ytterbium (III) (complex **3** in Scheme 1). The NLO behaviors of **3** and **4** are compared to that of La derivative (bis-{2(3), 9(10), 16(17), 23(24)-(tetrapyridin-4-yloxy phthalocyaninato)} lanthanum (III) (complex **2** in Scheme 1). The latter was highly aggregated in solution, but showed reasonable NLO behavior. The bulky pyridine substituents are expected to reduce aggregation, but this is not always the case as will be shown in this work.

This work presents the nonlinear optical properties of complexes **2**, **3** and **4** in solution and when embedded in poly (methyl methacrylate) (PMMA).

2. Experimental

2.1. Materials

1-Pentanol, lutetium (III) chloride and ytterbium (III) chloride hexahydrate were purchased from Sigma–Aldrich. Dimethyl formamide (DMF), dimethyl sulfoxide (DMSO) and poly (methyl methacrylate) (PMMA) were purchased from Merck. Tetrahydrofuran (THF) was purchased from MINEMA. 1,8-Diazabi cyclo[5.4.0]undec-7-ene (DBU) was purchased from Fluka. The synthesis of 4-(pyridin-4-yloxy)-phthalonitrile (**1**) was according to literature methods [18].

---

* Corresponding author. Tel.: +27 46 603 8801; fax: +27 46 622 5109.
E-mail address: t.nyokong@ru.ac.za (T. Nyokong).

http://dx.doi.org/10.1016/j.optmat.2015.05.022
0925-3467/

2.2. Synthesis of bisphthalocyanines

*2.2.1. Synthesis of bis-{2(3), 9(10), 16(17), 23(24)-(tetrapyridin-4-yloxy phthalocyaninato)} lanthanum (III) (**2**)*

Complex **2** was synthesized according to methods employed for other $LnPc_2$ complexes [19]. Briefly, compound (**1**) (215.7 mg, 0.975 mmol) and lanthanum chloride (29.89 mg, 0.122 mmol) were added to a round bottom flask. DBU (0.5 mL) and 1-pentanol (15 mL) were added to the reaction mixture, followed by heating under reflux for 21 h in open air to obtain a green product of **2**. Following centrifugation using THF, a green product was formed at the bottom of the centrifuge tube and was washed with methanol and THF (1:2). The obtained product was then introduced into a reverse phase column to give complex **2** after eluting with a mixture of DMF and THF (v/v; 3:1).

Yield: 26%. IR: [KBr, ν, cm^{-1}] 809, 825, 840, 825, 892, 1006 (Pc skeleton), 1046, 1072, 1111, 1136, 1158, 1225, 1244, 1286, 1316, 1496, 1530 (C—O—C), 1574, 1658, 1728 (—C=N—), 2856, 2924, 3068 (C—H, aromatic), 3291, 3397 (OH). UV–Vis (DMSO): λ_{max} nm ($\log \varepsilon$) 400 (4.36), 618 (4.46), 683 (4.78). Anal. Calc. for $C_{104}H_{56}N_{24}O_8La \cdot H_2O$: C, 64.83; H, 3.03; N, 17.45. Found: C, 64.13; H, 2.73; N, 16.69%. ^1H NMR (DMSO-d_6): δ, ppm 8.72–8.70 (2H, d, Ar—H), 8.19–7.56 (41H, m, Ar—H), 7.25–7.16 (2H, m, Ar—H), 6.79–6.77 (2H, d, Ar—H), 6.55 (1H, s, Ar—H), 6.30–6.14 (8H, m, Ar—H). MS (MALDI-TOF): (m/z): Calc. 1907 amu. Found: 1912 amu $[M + 5H^+]$.

*2.2.2. Synthesis of bis-{2(3), 9(10), 16(17), 23(24)-(tetrapyridin-4-yloxy phthalocyaninato)} ytterbium (III) (**3**)*

Complex **3** was prepared as described for complex **2** except that complex **1** (215.7 mg, 0.975 mmol) and ytterbium chloride hexahydrate (47.3 mg, 0.122 mmol) were employed. The product obtained was transferred to a centrifuge tube, followed by addition of THF. After centrifugation at 3500 rpm for several minutes, supernatant obtained was evaporated under reduced pressure, yielding a green product which was subjected to a column packed with silica and eluted with a mixture of DMF and THF (v/v; 2:3). After evaporation, the product was subjected to a reverse phase column to give complex **3** after eluting with a mixture of DMF and THF (v/v; 3:1).

Yield: 19%. IR: [KBr, ν, cm^{-1}] 663, 680, 750, 811, 847, 892, 974 (Pc skeleton), 1044, 1080, 1127, 1189, 1264, 1322, 1403, 1482, (C—O—C), 1562, 1633 (—C=N—), 2924, 3058 (C—H, aromatic), 3230 (OH). UV–Vis (DMSO): λ_{max} nm ($\log \varepsilon$), 354 (4.79), 621 (4.40), 687 (4.99). Anal. Calc. for $C_{104}H_{56}N_{24}O_8Yb$: C, 64.30; H, 2.91; N, 17.30. Found: C, 63.71; H, 3.13; N, 17.22%. ^1H NMR (DMSO-d_6): δ, ppm 8.47–7.69 (39H, m, Ar—H), 6.47–6.32 (17H, d, Ar—H). MS (MALDI-TOF): (m/z): Calc. 1943 amu. Found: 1947 amu $[M + 4H^+]$.

2.2.3. Synthesis of thin films

PMMA (200 mg) was added to DMF (2.5 mL) and the mixture stirred at room temperature in an airtight vial. Each of the $LnPc_2$ complexes (**2**, **3** or **4**; 1.65 mg) was transferred into a well dissolved PMMA solution and stirred for another 24 h. The mixture was then transferred onto a clean thin glass slide and dried in the oven at 110 °C. The thin films (TF) prepared from complexes **2**, **3** or **4** are presented as **TF-2**, **TF-3** and **TF-4**, respectively. Film thickness (~7 μm) was determined by utilization of the knife edge attachment of the Bruker D8 Discover X-ray diffraction (XRD) following removal of the films from the glass slides.

2.3. Equipment

Infrared spectra were recorded on a Perkin Elmer 100 ART FT-IR spectrometer. Ultraviolet–visible spectra (UV–Vis) were recorded on a Shimadzu UV–Vis 2550 spectrophotometer. The emission spectra were recorded on a Varian Cary Eclipse fluorescence spectrophotometer. Luminescence lifetimes were measured using time correlated single photon counting setup (TCSPC) (PicoQuant FluoTime 200). The excitation source was a diode laser LDH-P-670 with PDL 800-B, 670 nm and 20 MHz repetition rate Picoquant GmbH. Details have been provided before [20]. ^1H nuclear magnetic resonance (NMR) signals were recorded on a Bruker AMX 300 NMR spectrometer. Elemental analyses were carried out on a Vario EL III MicroCube CHNS Analyzer.

All Z-scan experiments described in this study were performed using a frequency-doubled Nd:YAG laser (Quanta-Ray, 1.5 J/10 ns fwhm pulse duration) as the excitation source. The laser was operated in a near Gaussian transverse mode at 532 nm (second harmonic), with a pulse repetition rate of 10 Hz and energy range of 0.1 μJ–0.1 mJ, limited by the energy detectors (Coherent J5-09). The low repetition rate of the laser prevents cumulative thermal nonlinearities. The beam was spatially filtered to remove the higher order modes and tightly focused with a 15 cm focal length lens. The Z-scan system size ($l \times w \times h$) used was 600 mm × 300 mm × 350 mm (excluding the computer, energy meter, translation stage driver and laser system). The liquid samples were placed in a cuvette (internal dimensions: 2 mm × 10 mm × 55 mm, 0.7 mL) and a path length of 2 mm (Starna 21-G-2). For thin films, no damage was detected between runs since the sample was moved or replaced.

Electron paramagnetic resonance (EPR) spectra were recorded on a Bruker EPR 300E X-band (10 GHz) spectrometer equipped with a TM probe with a flat quartz cell. The spin Hamiltonian parameters were obtained by simulation of the spectra. The static field (2000–3486.18 G), the modulation amplitude (6.09–6.23 G), the time constant (10.24 ms), the conversion time (5.12 ms), the resolution (2048 pts), power (2.00 mW), the modulation frequency (100 kHz) and the center field (3500 G) were used as the experimental parameters at 298 K using twenty–thirty scans.

2.4. Fluorescence quantum yields

Fluorescence quantum yields (Φ_F) were calculated using comparative methods described before [21,22] using ZnPc in DMSO as a standard: $\Phi_F^{Std} = 0.20$ [22].

2.5. Nonlinear optical parameters

Using nonlinear regression technique, all open aperture Z-scan data were fitted with Eqs. 1–3, in which the normalized transmittance ($T_{Norm}(z)$) is defined as a function of position [23–25] as described by Sheik-Bahae and co-workers.

$$T_{Norm}(z) = \frac{1}{\sqrt{\pi} q_0(z)} \int_{-\infty}^{\infty} \ln\left[1 + q_0(z) e^{-\tau^2}\right] d\tau \tag{1}$$

where

$$q_0(z) = \frac{\beta_{eff} I_0 L_{eff}}{1 + (z/z_0)^2} \tag{2}$$

where β_{eff} and I_0 are the effective intensity dependent nonlinear absorption coefficient and the intensity of the beam at focus respectively. L_{eff} is the effective thickness of the sample and is given by Eq. (3) [25,26]. z and z_0 are sample position with respect to the input intensity and Rayleigh length (defined by $\pi w_0^2/\lambda$; λ = wavelength of the laser beam and w_0 = beam waist at the focus ($z = 0$)), respectively.

$$L_{eff} = \frac{1 - e^{-(\alpha L)}}{\alpha} \tag{3}$$